Efficient Method of Detecting Blurry Images

Elena Tsomko, Hyoung Joong Kim, Joonki Paik, In-Kwon Yeo

Abstract—In this paper we present a simple, efficient method for detecting the blurry photographs. Recently many digital cameras are equipped with various auto-focusing functions to help users take well-focused pictures as easily as possible. In addition, motion compensation devices are able to compensate motion causing blurriness in the images. However, digital pictures can be degraded by limited contrast, inappropriate exposure, imperfection of auto-focusing or motion compensating devices, unskillfulness of the photographers, and so on. In order to decide whether to process the images or not, or whether to delete them or not, reliable measure of image degradation to detect blurry images from sharp ones is needed. This paper presents a blurriness/sharpness measure, and demonstrates its feasibility by using extensive experiments. This method is fast, easy to implement and accurate. Regardless of the detection accuracy, the proposed measure in this paper is not demanding in computation time. Needless to say, this measure can be used for various imaging applications including auto-focusing and astigmatism correction.

Index Terms—blur image, detection, variance.

1 Introduction

SHARPNESS measure has been used in many engineering and scientific applications including, for example, the auto-focusing applications for digital cameras, and astigmatism correction in the scanning electron microscope or the transmission electron microscope [2], [6]. Note that the images taken by microscopes are, generally, well structured than digital photos. The former images may contain much more texture regions than the latter ones. Thus, the sharpness metrics for the former ones mainly focus on the sharp edges separating texture regions. However, needless to say, the sharpness metrics can be applied to any digital photos. The main objective of this paper is detecting blurry photos from sharp ones taken by digital cameras. Nowadays, high-quality digital cameras gain increasing attention as digital technology advances. Users can take hundreds of pictures a day. However, it is not easy for them to look through all their pictures. When their storage is full, they have to delete some images with poorer quality. Thus, they need measures of image quality for telling the blurry images from the sharp ones. Basically, they prefer sharp images to blurry ones unless they prefer these images intentionally. Based on the image metrics, the machine can automatically delete images with poor quality or make a list of such images so that users can have a look and choose what to delete. On the other hand, computers can make them automatically go through an enhancement process for better quality. Typical causes of blurriness include: out-of-focus, camera jitter, moving objects, limited contrast, inappropriate exposure, and so on. However, imperfect focusing and/or motion is the main source of blurriness in the digital photographs. In this context, the measure of blurriness/sharpness takes the Gaussian and motion blurriness into consideration.

One potential problem of the measures is their false positive or false negative decisions. Some images actually not blurry can be perceived to be blurry or blurry images to be sharp

- *Elena Tsomko is a Ph.D. student at the Department of Information Management and Security, Korea University, Seoul, Korea, 136-701.*
  E-mail: elena@korea.ac.kr
- *Hyoung Joong Kim is a full professor at CIST, Korea University, Seoul, Korea, 136-701.*
  E-mail: khj-@korea.ac.kr
- *Joonki Paik is a full professor at Image Processing and Intelligent Systems Laboratory, Graduate School of Advanced Imaging Science, Chung-Ang University, Seoul, Korea, 156-756*
- *In-Kwon Yeo is an Associate Professor, Department of Statistics, Sookmyung Women's University, Seoul, Korea, 140-742*

Manuscript received February 15, 2008; revised March 20, 2008.

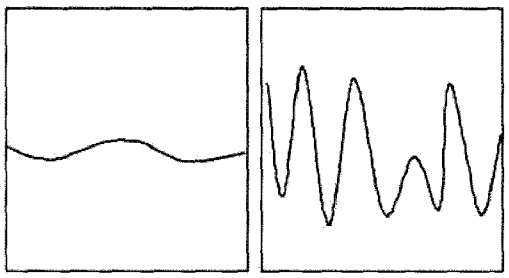

Fig. 1. Conceptual illustration of blurry (left) and sharp (right) images

images. The sharp images perceived to be blurry include, for example, foggy landscapes, scenes with cloudy sky, and so on. Images of sands, sea, or fields with unclear edges look blurry even though they are sharp. In addition, filtering or compression can cause blurriness. On the other hand, blurry images perceived to be sharp include large plain planes with clear edges. Note that human decisions can be arguable. Sometimes, the divide between two categories is unclear and subjective. Thus, it is not easy to say that image classification based on the sharpness/blurriness measures can be perfect.

Even with reasonable performance of auto-focusing and/or motion compensation algorithms image degradation is unavoidable unless entire robustness is guaranteed in the system [10]. In order to automatically select blurry pictures among a pool of digital pictures, various measures of sharpness or blurriness have recently been proposed [5], [10], [11], [13], [14], [15], [16], [20]. The simplest measure is the ratio of high frequency components to low frequency components. Blurry pictures tend to become smoother than crisp images, and contain less number of edges as illustrated in Figure 1.

As shown in Figure 1, blurry pictures may have smaller gradients in the edge regions and less energy in high frequency components. Thus, images are usually transformed by DCT or DWT, and are quantized to see how much high frequency components exist. Some simple approaches count occurrence of non-zero DCT coefficients [12]. Larger number of non-zero coefficients means that the image is sharper. Sum of high-frequency components larger than the threshold value [9] also plays the similar role.

As shown in Figure 1, blurry pictures may have smaller number of grey-level values than sharp ones. Thus, counting number of bins in the histogram of the grey-level values can be a good solution [9]. It is assumed that a sharper image has a larger number of bins. Extreme case is the uniformly distributed histogram with maximum number of bins. In the same context, entropy can be used to measure sharpness. If the probability of occurrence of each grey-level is low, the entropy is high and vice versa. In other words, a sharp image has high entropy. The probability distribution can be a good indicator of sharpness. Sharper image has larger variance [6] or larger kurtosis [21] values.

As shown in Figure 1, blurry images are highly correlated while sharp images are not. Thus, auto-correlation [2] can be a good metric for sharpness. Derivatives [4] can be the other good indicators. For example, the first-order derivative (i.e., gradient) which acts as a high-pass filter can be a good indicator. Sharp images have large derivative values.

On the other hand, wavelet-based blurriness/sharpness estimation methods have been proposed in [11], [14], [18]. For example, Rooms et al. [15] have proposed the Lipschitz exponent-based method which suits well only for medical applications such as microscope images of cell nuclei. Ferzli and Karam [7] propose a sharpness measure based on the Lipschitz regularity for differentiating between edges and noise singularities. This metric performs quite well when dealing with a moderately noisy environment. On the other hand, special characteristics of human visual system can be exploited to provide reasonable sharpness metric [8].

Batten et al. [3] evaluate the gradient measure, auto-correlation measure, frequency-domain measure, and variance measure, and conclude that the last measure is better than others in terms of computing time and immunity to noise. The gradient measure is most

susceptible to noise, while the variance measure is largely insensitive. The auto-correlation measure is usually strictly unimodal, but has poor reproducibility. Reproducible measure has a sharp peak. A strictly unimodal sharpness measure has a single peak at the best focus and monotonically decreasing away from this peak. The implementation cost of the frequency-domain measure is significant. A fair comparison of various methods is available in [7].

Most of the aforementioned methods aim at auto-focusing and astigmatism correction. On the other hand, to make better classification of pictures in the sense of sharpness many measures have additionally been proposed. A good measure should be invariant to pictures and picture contents, and well correlate with perceived sharpness. Shaked and Tastl [16] have developed an algorithm to estimate the overall sharpness of a picture to determine how much sharpening should be applied to each picture. They estimate the global sharpness of a picture by a single scalar value. However, the single value criterion could not provide sufficiently invariant measure with various pictures. In order to solve this problem Banerjee et al. [1] have segmented pictures based on the rule-of-thirds to exploit local features. Lim et al. [10] have developed an effective, efficient algorithm which uses several global figure-of-merits computed from local image statistics. Thus, one can see that many measures have been proposed for images' quality estimation, nevertheless, they are mostly applicable to microscope images, and those methods for digital photos are computation-intensive and/or include complex parameters to be estimated.

In this paper, we propose a new measure based on computing the prediction residue between neighboring pixels in the images and computing variance to measure the sharpness or blurriness without reference. This measure is totally different from the previous variance measure [6]. Previous measure computes variance of the pixel values themselves, while the proposed measure computes variance of the prediction residue of neighbor pixels. We also propose a criterion to decide whether the image is sharp or blurry. This paper shows why the proposed measure is mathematically reliable, easy to implement, and fast. In addition, the feasibility of the proposed measure is shown with thorough experiments with various images. Regardless of the detection accuracy, existing measures are computation-intensive. However, the proposed measure in this paper is not demanding in computation time. For this measure, transform is not necessary. Complex and time-consuming operations are not requested. Computing prediction residue for P random sample pairs and computing variance are sufficient, where P is approximately 300 among $M \cdot (N-1)$ sample population for an $M \times N$ sized image. The prediction operator is just computing difference between adjacent pixels. In addition, accuracy of the proposed measure is very high.

2 Theoretical Background

2.1 Previous Variance Measure

The variance of an image is a good measure of sharpness [6]. However, its performance needs to be further improved. The variance for sharpness measure of Erasmus and Smith [6] in the spatial-domain is defined as follows:

$$\sigma^2 = \frac{1}{MN}\sum_{x=1}^{M}\sum_{y=1}^{N}[u(x,y)-\bar{u}]^2, \qquad (1)$$

where $\bar{u}$ represents the mean intensity of $u(x,y)$. They compute the global variance of the whole pixel values in the spatial domain. However, note that the distribution, i.e., histogram of a real image is, in general, neither Gaussian nor Laplacian. On the other hand, real images are highly correlated. The variance measure in Equation (1) does not take this correlation into account.

Figure 2 shows an original, sharp Baboon image (top) and its blurred versions: the motion blurred (center) and Gaussian blurred (bottom) images as well. Their histograms are shown in Figure 3. It is obvious that the sharp image histogram (solid line) is flatter than the histograms of the blurred images (dashed lines in top and bottom images of in Figure 3). The standard deviations of the original and, for example, Gaussian blurred images are 1,808 and 1,022, respectively. Note that large difference between

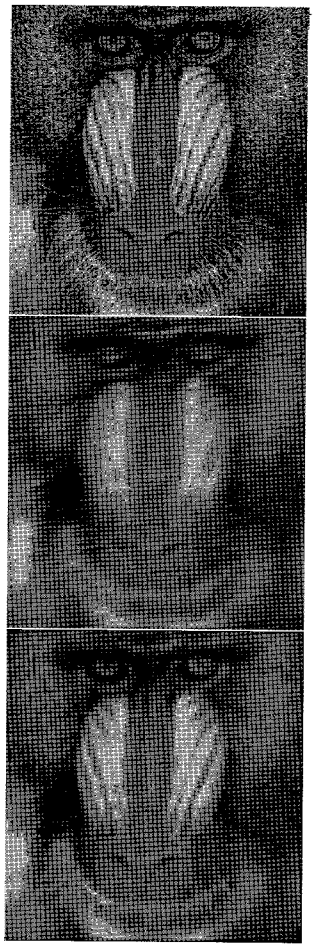

Fig. 2. The original Baboon image (top), its motion-blurred (center) and Gaussian-blurred images (bottom)

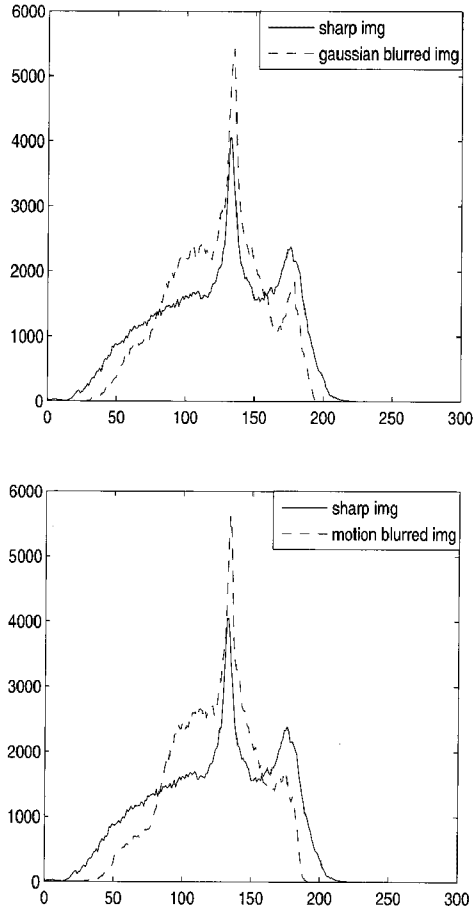

Fig. 3. Distribution of grey-level values of the original Baboon image (solid line) and its Gaussian-blurred image (dashed line) (top), and the original Baboon image (solid line) and its motion-blurred image (dashed line) (bottom)

those two figures is desirable for the point of image classification. However, in this case, the ratio is around 1.8 (i.e., 1,808/1,022).

2.2 New Variance Measure

In general, images are highly correlated. When there is significant correlation between successive samples, it should be possible to predict the value of any given sample with a reasonably high degree of accuracy from some of the preceding samples. The difference between the actual image and its predicted version is often called prediction residue or prediction error. If the prediction algorithm is reasonably good, most of the values in the residue will be zero or very close to it. This in turn means that the distribution function of the predicted signal will be peaky. It is the decorrelation process in the image compression. When the image is decorrelated, its distribution is nearly Gaussian or Laplacian-like [19].

There are many decorrelators available in the literature [17]. The simplest predictor for an image is the one that uses the previous pixel, $u(x, y-1)$, in the image as the predicted value, $\hat{u}(x, y)$, of the current pixel, $u(x, y)$. Formally,

if we denote the current pixel by $u(x,y)$ and the previous pixel by $u(x,y-1)$, the prediction $\hat{u}(x,y)$ of $u(x,y)$ is given by $\hat{u}(x,y) = u(x,y-1)$. In this case, the prediction residue, $g(x,y)$ is nothing but a difference between the adjacent pixels. Hence, $g(x,y) = u(x,y) - \hat{u}(x,y) = u(x,y) - u(x,y-1)$.

Let ρ be the coefficient of correlation between $u(x,y-1)$ and $u(x,y)$. Suppose that relationship between $u(x,y-1)$ and $u(x,y)$ can be expressed as $u(x,y) = \rho u(x,y-1) + \varepsilon(x,y)$, where $\varepsilon(x,y)$ denotes a white noise and is uncorrelated with $u(x,y-1)$. Then, the variance of $g(x,y)$ is

$$var\{g(x,y)\} = var\{(\rho-1)u(x,y-1) + \varepsilon(x,y)\},$$

or

$$var\{g(x,y)\} = (\rho-1)^2 var\{u(x,y-1)\} + var\{\varepsilon(x,y)\}.$$

Note that, in general, $var\{\varepsilon(x,y)\}$ is much smaller than $var\{g(x,y-1)\}$ except edges in images. Experiments show that ρ of the blurred images tends to be larger than that of the original images. As shown in Figure 3, the number of edge points of the original Baboon image is relatively larger than that of the blurred image. These imply that the blurred image has much smaller variance of $g(x,y)$ than the original does.

Figure 4 shows the histogram of the differences between adjacent pixels for the original Baboon image (solid line) and its Gaussian and motion-blurred versions (dashed lines in top and bottom pictures, respectively). Comparing this with Figure 3, we can see that even a simple predictor like this can generate a histogram that is significantly informative. The standard deviations of the original and, for example, Gaussian-blurred images are 206.6 and 3.1, respectively. In this case, the ratio is around 66.6 (i.e., 206.6/3.1), which is much higher than that obtained in Figure 3. With more sophisticated predictors, one can expect better performance. The variance figures are computed by Equation (1) and Equation (2) to be given later.

Note that the histogram of the pixel values themselves in Figure 3 and that of the prediction residues in Figure 4 are obviously distinctive. The former distribution is neither Gaussian nor Laplacian-like. On the other hand, the latter distribution is very close to Gaussian or Laplacian. Thus, the variance of the latter one is more meaningful since variance is a good parameter for characterizing the Gaussian distribution. Moreover, the ratios between original image and blurred one are also apparently different. The large ratio assures certainty in detecting the sharp images from the blurry images.

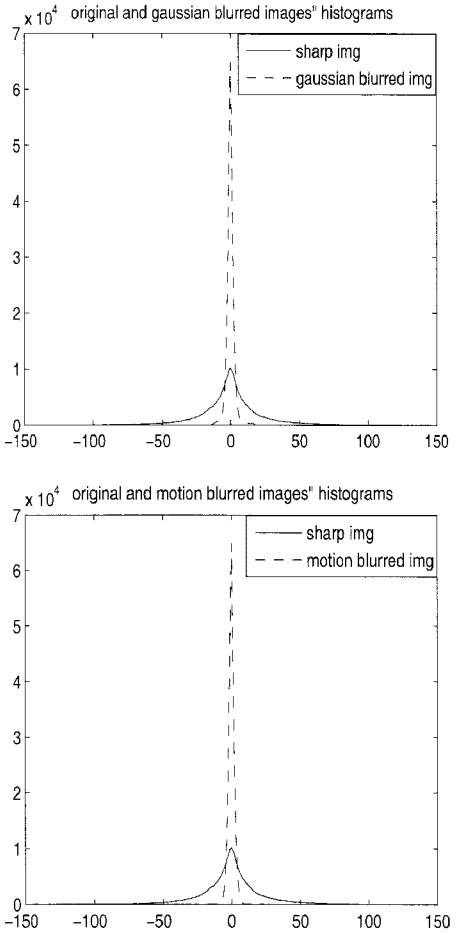

Fig. 4. Distribution of prediction residues of the original Baboon image (solid line) and its Gaussian-blurred image (dashed line) (top), and original Baboon image (solid line) and its motion-blurred image (dashed line) (bottom)

The variance for sharpness measure using the residue prediction is defined as follows:

$$\sigma_p^2 = \frac{1}{M(N-1)} \sum_{x=1}^{M} \sum_{y=1}^{N-1} [g(x,y) - \bar{g}]^2, \quad (2)$$

where $\bar{g}$ represents the mean of $g(x,y)$'s. Equation (2) can be rewritten with different predictor or different organization scheme of the prediction residue. Let g be the prediction residue vector. Then, the prediction residue vector can be modeled as Laplacian distribution as follows:

$$f_g(g) = \frac{\sigma_l}{2} e^{-\sigma_l |g|}, |g| < \infty \quad (3)$$

The best dispersion measure for the Laplacian-like distribution is

$$\sigma_l^2 = \frac{1}{M(N-1)} \sum_{x=1}^{M} \sum_{y=1}^{N-1} \left| g(x,y) - \tilde{g} \right|,$$

where $\tilde{g}$ stands for the median of $g(x,y)$'s. However, we need a heavy computing time to figure out σ_l^2 since a sorting algorithm should be applied to compute the median $\tilde{g}$.

Hence, we employ the sample variance value S_p^2 as the measure of sharpness for both Gaussian and Laplacian distribution. Computing variance value, σ_l^2 or σ_p^2, using all pixels is time-consuming. In addition, the accuracy of such variance is not so satisfactory. Thus, in this paper, we just compute the sample variance value, S_p^2, using P sample pixels. We randomly select P pixels from the two-dimensional pixel array $u(x,y)$ and allocate them to the one-dimensional array, $v(k)$, $k = 1, \cdots, P$. Thus, the sample variance value, S_p^2, is computed as follows:

$$S_p^2 = \frac{1}{P} \sum_{k=1}^{P} [v(k) - \bar{v}]^2. \quad (4)$$

From a set of test images the sample variance values are listed in Table 1. The figures are different from filter to filter, resolution by resolution, camera by camera, and so on. The figures in Table 1 are obtained by using Gaussian low-pass filter with MATLAB *fspecial* function. In order to reduce the computation time considerably, we take 300 sample pairs randomly and compute the measure based on the prediction residue of the sample pairs. The number of sample pairs, P, is adjustable to such a value that meets requirements of computing time and accuracy of the detection.

TABLE 1
Variances of a set of standard test images: sharp ones and their blurred counterparts

Images	S_p^2 of sharp image	S_p^2 of blurred image
Baboon	206.6	3.1
Lena	61.9	4.4
Peppers	10.2	3.5
Peppers2	47.1	4.8
Sailboat	65.9	7.6
Tiffany	68.9	3.8

As shown in Table 1, the sample variance of the sharp Baboon is 206.6 while that of the blurred image is just 3. The sample variances of the blurred images mostly depend on the degree of the blurriness. More blurred images may have smaller sample variance values, and less blurred ones have larger sample variances. The sample variance figures in Table 1 are obtained from the sharp and blurry images. The latter ones are artificially blurred versions of the corresponding sharp images. Note that these figures justify our assumption.

As it is aforementioned, the single measure cannot be sufficiently invariant to various pictures. That is why we propose to use three measures: the sample variance value S_p^2 for the global sharpness measure, the variance value σ_b^2 for the local sharpness measure, and the ratio of the sharp subblocks to the tested subblocks, R_s, for the local sharpness measure. In addition, we need three pairs of threshold values: two pairs of local threshold values t_1, t_2, V_1, and V_2; and one pair of global threshold values T_1 and T_2. The main role of the global threshold values is to decide whether the image is globally sharp or not. For example, the Baboon image (see Table 1) has a large sample variance value, 206.6, that exceeds the first threshold value (i.e., $T_1 = 100$, which can be decided by the users based on their applications and requirements). Thus, the image is identified as the globally sharp one. However, decision making based on a single global measure may cause

large false negative or false positive errors. As one can see, other images have sample variance values smaller than T_1, even though they are sharp. Of course, the threshold value can be reduced to allow these images to be decided as sharp. However, decreasing the threshold values will incur additional unintended consequences. When the sample variance values are smaller than the threshold value, the image needs to be analyzed locally to see if it is really blurry or not. Images may be decided to be globally blurry, but actually sharp because they are locally sharp.

Thus, local variance value

$$\sigma_b^2 = \frac{1}{m(n-1)} \sum_{x=1}^{m} \sum_{y=1}^{n-1} [g(x,y) - \bar{g}]^2, \qquad (5)$$

need to be used to achieve much better performance. Images can be divided into $m \times n$ non-overlapping subblocks. The local variance value for p subblocks can be used as a good indicator for local sharpness or blurriness of the image. A block having large variance value may be locally sharp. On the other hand, a block with small variance value may be locally blurry. These local variance values are very useful for categorizing the images in detail.

According to the proposed method, the images can be classified into four categories:

- Globally sharp images: The global sample variance value S_p^2 of this kind of images is generally very large. The Baboon image is a good example. This image is full of high-frequency components. Thus, when the global variance value is very large, it is safe to categorize the image as globally sharp one. The local variance values σ_b^2 of this kind of images are most likely to be large. However, we don't need to compute the local variance values because this category of images are certainly globally sharp in general.

- Sharp images with locally blurry subparts: This kind of images may have a global variance value S_p^2 not so large. Even though the global variance values of Lena, Tiffany, and Airplane are much less than T_1, they are sharp. Another good example for this category is Peppers. This image is full of plain textures in the rinds which make these regions look blurry. This fact can be proven with the local variance values σ_b^2. Note that most of the local variance values of this kind of images are large.

- Apparently globally blurry images with locally sharp subparts: This kind of images may have a global sample variance value smaller than T_1. Especially, the sport photos with high motion blurs in the background are included in this category. Such images can be classified as partially blurry images as they are. However, some parts (and these are, generally, sharp parts) of this kind of images will have large local variance values. Otherwise, this kind of images should be classified as globally blurry. Images of mostly sky, clouds, sea, sands, snow with or without small objects in the scene will look apparently sharp in human eyes. However, this kind of images may not be categorized as sharp images. This kind of false decision should be avoided.

- Globally blurry images: The global sample variance values of these images are generally very small. In addition, the local variance values of this kind of images will be mostly small.

Thus, in order to make better algorithm, the global and local variance values as well are exploited in this paper.

2.3 Algorithm

The core of the proposed algorithm is its proper image quality measures and the appropriate threshold values for making reliable decisions. The measure is the sample variance of the prediction residues of P sample pairs among $M \cdot (N-1)$ population. Through the extensive experiments we found that 300 sample pairs would be enough for computing eligible vari-

ance values. Note that, since $P \ll M \cdot (N-1)$, computation time of the proposed measure is notably insignificant. Deciding the threshold values for evaluation of the local variance values is another key of success of the algorithm. Fixed threshold values for all images may cause high false alarm rate for a certain type of images. Thus, we propose to use the flexible threshold values for different applications and requirements.

As a preprocessing, we only need to convert the input images from RGB colors to grey-level luminance values. The resolutions of the digital cameras in these experiments are either $960 \times 1,280$, $1,200 \times 1,600$, or $1,536 \times 2,048$.

Detection algorithm based on the new measures can be summarized as follows (see the block-scheme on Figure 5):

I Take P sample residue values randomly, and compute the sample variance value S_p^2.

II If $S_p^2 > T_1$, then the image is identified as a globally sharp one. In this case, stop evaluation. Otherwise, divide the image into non-overlapping subblocks of size $m \times n$ and compute the local variances σ_b^2 for each one using the same amount $p = P$ of difference sample residues. After getting the p variance values of the subblocks, obtain the local threshold value t_1 by taking average value of all the variances σ_b^2 such as

$$t_1 = \frac{1}{p}\sum_{x=1}^{p}(\sigma_b^2)_x, \qquad (6)$$

where $(\sigma_b^2)_x$ denotes the variance value of the xth subblock, disregarding those ones that have very large values (if only there are not many of them).

III Evaluate the sample variance value S_p^2 to see if it is larger than the global threshold value T_2, then compute the number of blocks with $\sigma_b^2 < t_1$. If the ratio of such blocks to all the subblocks, R_s, is less than V_1, then the image is identified as a globally sharp one. Otherwise, it is an average quality image that may contain some blurry parts (i.e., moving objects, or blurry background, etc.), or can be taken with insufficient exposure.

IV If the global variance S_p^2 is smaller than the global threshold T_2, then the image should be checked if it is globally blurry by computing the number of blocks with $\sigma_b^2 < t_2$. If $R_s > V_2$, i.e., if there are more than $V_2\%$ of such blocks, then the image is identified as a globally blurry one. Otherwise, go to Step III from the part for computing the number of blocks with $\sigma_b^2 < t_1$.

Thus, as one can see, we use three pairs of the thresholds in the algorithm. They are the global threshold values (i.e., T_1 and T_2), the local ones, (i.e., t_1, t_2), and the ratios thresholds for local sharpness (i.e., V_1 and V_2). Through the extensive experiments we find that mostly the sharper image has a larger variance value. However, it is impossible to use only one fixed global threshold T_1 for evaluation of all the images since sometimes globally sharp images can have smaller variance value due to the special properties of them. In the experiments, we conclude that the value $T_1 = 100$ is a good threshold value that only globally sharp images can exceed. The threshold value $T_2 = 60$ is decided such that globally blurry images do not exceed. Thus, to tell globally sharp and average images from the globally blurry ones we need some additional criteria. They are the ratio R_s with the local variance values smaller than t_1 or t_2. If more than V_1 percent of blocks have the local variance values smaller than t_1, then the images can be identified to be of average quality: i.e., they are neither clearly sharp nor seriously blurry. Otherwise, it can be either globally sharp or blurry image. The threshold t_1 is obtained automatically from the image itself (see Step II in the proposed algorithm). As for the threshold t_2, we propose the value 10 because mostly the blocks of really blurry images have variance values in the range from 0 to about 5.0. But to be sure we put $t_2 = 10$.

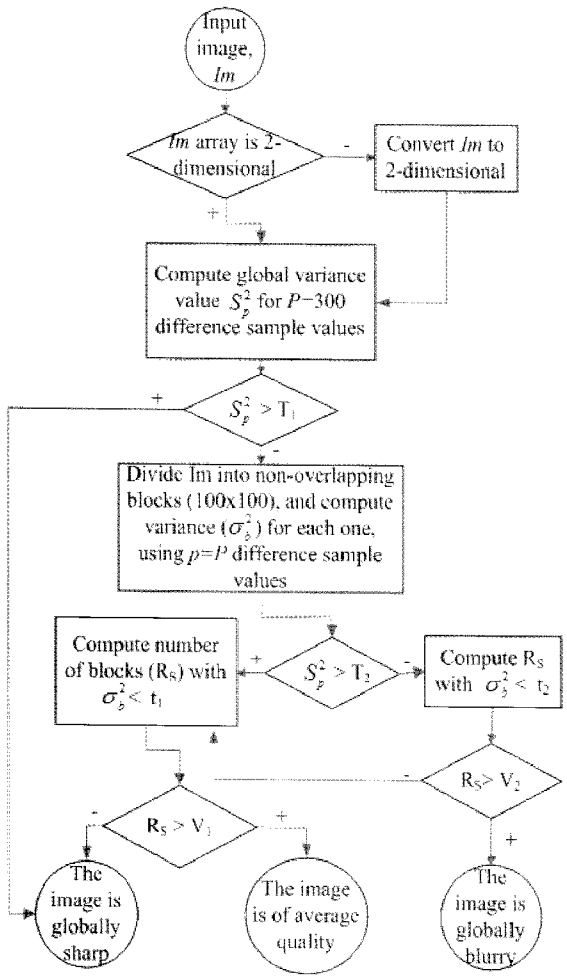

Fig. 5. Block scheme of the algorithm for the measure proposed in this paper

And if more than 70% of the blocks have such low variance values smaller than 10, then the image is identified as the globally blurry one.

3 Experiments

For the first experiment we take 140 photographs taken by a digital camera of spatial resolution 960×1,280. Among them 70 images are realistically blurry, and the rest of them are globally sharp. For the second test, 200 sharp color photographs of spatial resolution 1,536×2,048 are taken (almost all of them are sharp). To simulate their blurriness we add artificial blurriness to these images using Gaussian and motion filters with the same parameters of blurriness for all the images. The *fspecial* MATLAB function is used for the blurring. An example of intentionally blurred 400 images and their original counterpart 200 images is shown in Figure 6. As a result, we test 740 images (140 images plus 200×3 images).

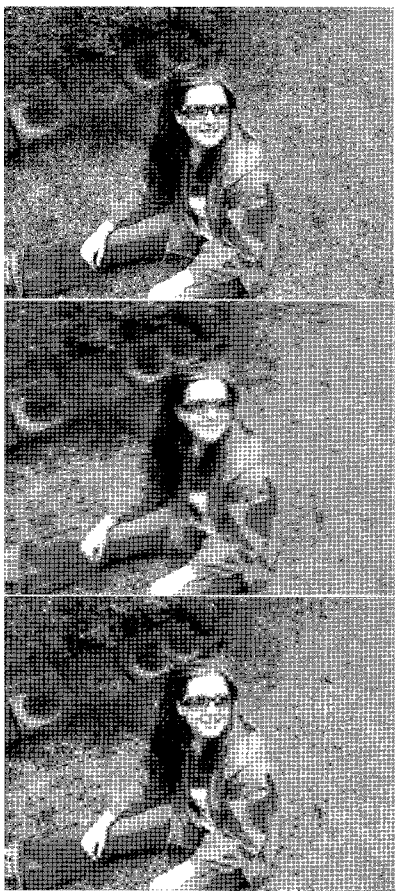

Fig. 6. The original image (top), motion-blurred image (center), and the low-pass filtered image (bottom)

In these experiments that use both sets of test images we compute variances (see Figure 7) with $P = 300$ sample pairs from $M \cdot (N-1)$ sample population. The horizontal axis

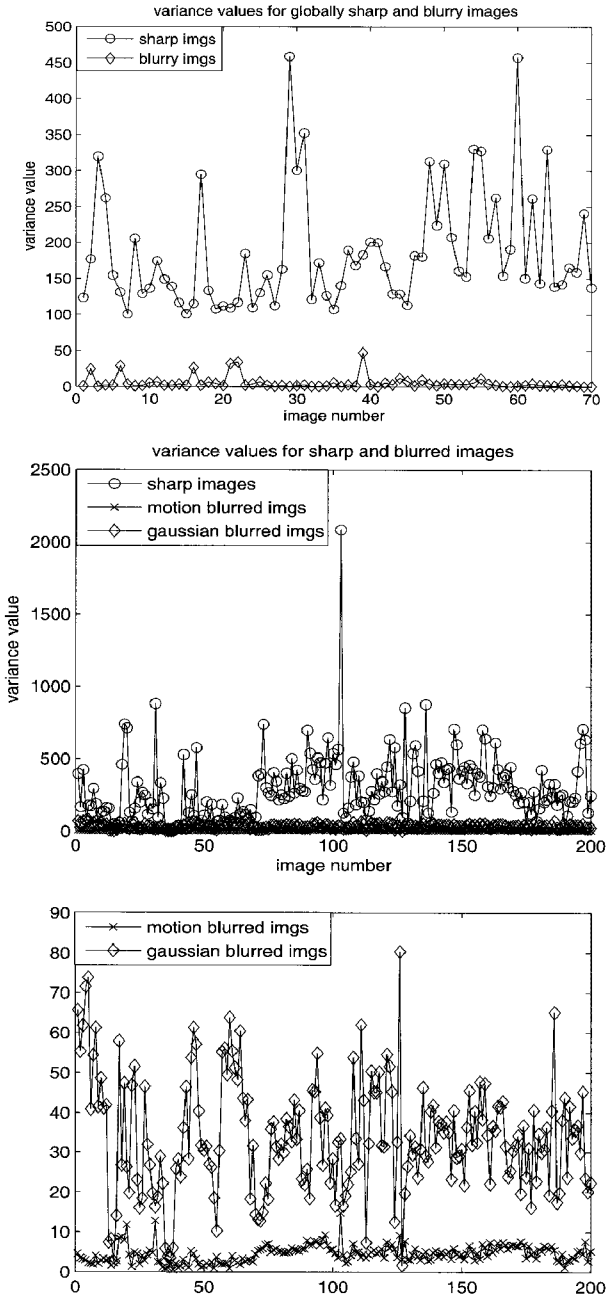

Fig. 7. Variances of 140 images (top) with 70 sharp ones (circled line) and 70 blurry ones (line with diamonds), those of 600 images (center) with 200 sharp (circled line), 200 motion-blurred (line with crosses), and 200 low-pass filtered ones (line with diamonds) computed using the measure proposed in this paper; and separate plots of variances for motion and Gaussian-blurred images (bottom)

shows the image number while the vertical axis shows the variance value of each image. As is expected, the sharp images (top line) have larger variances than blurry ones (bottom lines). However, it is not easy to decide an appropriate threshold value that can perfectly separate the sharp images from the blurry ones due to impulsive outliers. Thus, a single measure with a single threshold value may not tell blurry images from sharp ones perfectly. In these experiments, we select several parameters through thorough tests, and experimental results show that they are less sensitive to these parameters.

As a conclusion, based on the proposed algorithm we detect 98.15% of sharp images (265 from 270 sharp images where 70 sharp images are taken from the first test and 200 images are taken from the second test).

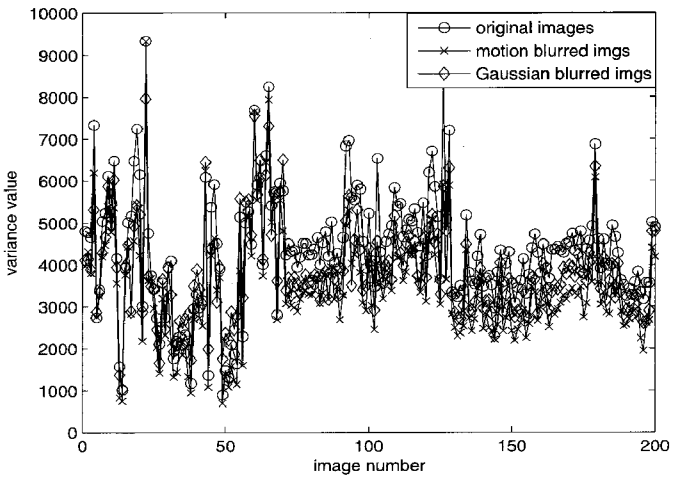

Fig. 8. Variances of 600 images with 200 sharp (solid line), 200 motion-blurred (line with crosses), and 200 low-pass filtered ones (line with diamonds) computed using [6]

The similar experiments have been done using the variance values [6] to compare results. We compare with their method because they also use variance values for evaluation of the images, but those values are obtained from the original images pixels' values, not from the differences between them. The original 200 images and the blurred versions of them are used for the experiments (the same amount

of blurriness has been added as for the previous test). As shown in Figure 8, note that the distance between circled line (for original images) and lines with crosses and diamonds (for blurred images) is very close compared with Figure 7.

Since the gap is very close, it is extremely difficult to tell good quality images from the bad ones. In this experiment, with method proposed in [6], we set the threshold value T for their method to be 4,000 (as variances are obtained from the spatial-domain pixel values). Then, among 197 original really sharp images, 122 are detected as the sharp images (see Table 2). Note that no threshold values are used in their method. This threshold value is used here just for comparing the detection ratio.

The same experiment has been done using the method proposed by S. Lim. This method in [10] outperforms method using spatial-domain variance values [6]. However, regardless of high accuracy of detection ratio in method proposed by [10], procedure is still highly computation-intensive. Disregarding this fact, their method seems to be excellent in terms of accuracy. Table 2 shows that our method produces very low false alarm rate compared with other methods. The only false detection case happens for the sharp images declared as blurry.

TABLE 2
Number of false alarms of three methods

Number of false alarms among 200 images	Ours	[6]	[10]
Sharp images declared to be blurry	3	78	28
Motion-blurred images declared to be sharp	0	50	18
Gaussian-blurred images declared to be sharp	0	66	24

For additional experiments with our method we take 4 more sets of 200 color images in each. There are different kinds of photographs in these sets: globally sharp, out-of-focus, images with insufficient exposure, motion blurred, noised images, etc. The resolutions of the photographs also vary: $960 \times 1,280$, $1,200 \times 1,600$, or $1,536 \times 2,048$. The contents in the Set #1 to #4 are a potpourri of outdoor, indoor, landscape, far, close, building photos, and so on. The detection ratio in Table 3 shows that our detection ratio is very high.

TABLE 3
Detection rate of globally blurry images for additional experiments

Image set	Detection rate	Image description
Set #1	100.0%	Outdoor, people
Set #2	100.0%	Outdoor, landscapes, views of city
Set #3	93.8%	Indoor, at party, at dinner
Set #4	98.8%	Outdoor, at concert

Based on the experiments we can conclude that the proposed measure is very simple and efficient. Unfortunately, there are few images that induce wrong decision. These images contain flat, monotonous areas that produce a large number of blocks with small variance values.

Totally, in our experiments we used more than 3,400 color digital images (1,140 original images and their blurred variants), and the average detection accuracy of the globally blurry images is 98.15%. The values of parameters in this paper are: $P = 300$, $m = 100$, $n = 100$, $T_1 = 100$, $T_2 = 60$, $t_2 = 10$, $V_1 = 50$ percent, and $V_2 = 70$ percent. Note that t_1 is adaptively computed according to images using Equation (6).

4 Discussions and Conclusion

It is worthwhile to point out that the notion of sharpness depends on the situation and an observer [10]. Sometimes people intentionally take pictures with intrinsically untextured objects such as snow or sky. We also take partially blurry pictures by adjusting depth of focus for special effects such as a photo of bees on a little blurry petals. Thus, it is difficult to give a golden rule that perfectly discriminates good and bad images. Although the points of view may be subjective, blurriness/sharpness measures are necessary for modern digital imag-

ing devices. Even though, recently, many digital cameras are equipped with various auto-focusing and motion compensating functions, however, the blurry pictures are unavoidable.

The proposed measure is fast, simple and efficient. Only P sample pairs are used for computing the measure among $M \cdot (N-1)$ sample population for global decision. In addition, for refinement of the decision, p subblock images are used for local measure. Every decision is made based on the sample variance value or the local variance values. In this paper, the main target of the proposed measure is detecting globally sharp and globally blurry images from a pool of digital photographs. Needless to say, this measure can be used for various imaging applications including auto-focusing and astigmatism correction.

ACKNOWLEDGMENTS

This research was supported by Korean Ministry of Information and Communication under the project funded by Information Technology Research Center (ITRC).

REFERENCES

[1] S. Banerjee and B. Evans, *Unsupervised automation of photographic composition rules in digital still cameras*, Proceedings of SPIE, vol. 5301, pp. 364-373, 2004.

[2] C. F. Batten, *Autofocusing and Astigmatism Correction in the Scanning Electron Microscope*, M.Ph. Thesis, University of Cambridge, 2000.

[3] C. F. Batten, D. M. Holburn, B. C. Breton, and N. H. M. Caldwell, *Sharpness search algorithms for automatic focusing in the scanning electron microscope*, Proceedings of SCANNING, 2001.

[4] A. Bovic, Ed. *Handbook of Image and Video Processing*, Academic Press, 2000.

[5] Y. Chung, J. Wang, R. Bailey, S. Chen, and S. Chang, *A non-parametric blur measure based on edge analysis for image processing applications*, IEEE Conference on Cybernetics Intelligent Systems, pp. 356-360, 2004.

[6] S. J. Erasmus and K. C. A. Smith, *An automatic focusing and astigmatism correction system for the SEM and CTEM*, Journal of Microscopy, vol. 127, pp. 185-189, 1982.

[7] R. Ferzli and L. J. Karam, *No-reference objective wavelet based noise immune image sharpness metric*, IEEE International Conference on Image Processing, vol. 1, pp. 405-408, 2005.

[8] R. Ferzli and L. J. Karam, *A human visual system-based no-reference objective image sharpness metric*, IEEE International Conference on Image Processing, 2006.

[9] L. Firestone, K. Cook, K. Culp, N. Talsania, and K. Preston, *Comparison of autofocus methods for automated microscopy*, Cytometry, vol. 12, pp. 195-206, 1991.

[10] S. Lim, J. Yen, and P. Wu, *Detection of out-of-focus digital photographs*, Technical Report, HPL-2005-14, 2005.

[11] S. Mallat and W. Hwang, *Singularity Detection and Processing with Wavelets*, IEEE Transactions on Information Theory, vol. 38, no. 2, pp. 617-643, 1992.

[12] X. Marichal, W. Y Ma, and H. J. Zhang, *Blur determination in the compressed domain using DCT information*, Proceedings of the IEEE International Conference on Image Processing, pp. 386-390, 1999.

[13] P. Marziliano, F. Dufaux, S. Winkler, and T. Ebrahimi, *A no-reference perceptual blur metric*, Proceedings of the International Conference on Image Processing, vol. 3, pp. 57-60, 2002.

[14] F. Rooms, A. Pizurica, and W. Philips, *Estimating image blur in the wavelet domain*, Proceedings of the Asian Conference on Computer Vision, pp. 210-215, 2002.

[15] F. Rooms, M. Ronsse, A. Pizurica, and W. Philips, *PSF estimation with applications in autofocus and image restoration*, Proceedings of the IEEE Benelux Signal Processing Symposium, pp. 13-16, 2002.

[16] D. Shaked and I. Tastl, *Sharpness measure: Towards automatic image enhancement*, Technical Report, HPL-2004-84R-2, 2005.

[17] P. Symes, *Digital Video Compression*, McGraw-Hill, 2004.

[18] Y. Y. Tang, L. Yang, and L. Feng, *Characterization and detection of edges by Lipschitz exponents and MASW wavelet transform*, Proceedings of the 14th International Conference on Pattern Recognition, vol. 2, pp. 1572-1575, 1998.

[19] M. J. Weinberger, G. Seroussi, and G. Sapiro, *The LOCO-I lossless image compression algorithm: Principles and standardization into JPEG-LS*, IEEE Transactions on Image Processing, vol. 9, no. 8, pp. 1309-1324, 2000.

[20] B. Zhang, J. Allebach, and Z. Pizlo, *An investigation of perceived sharpness and sharpness metrics*, Proceedings of SPIE, vol. 5668, pp. 98-110, 2004.

[21] N. Zhang, A. E. Vladar, M. T. Postek, and B. Larrabee, *A kurtosis-based statistitcal measure for two-dimensional processes and its application to image sharpness*, Proceedings of Section of Physical and Engineering Sciences of American Statistical Society, pp. 4730-4736, 2003.

Elena Tsomko graduated from Birobidjan State Pedagogical Institute, Department of Mathematics and Computer Science, Russia, 2004, received an M.S. degree in Multimedia Communications Engineering from Kangwon National University, Korea, in 2007, and is currently pursuing a Ph.D. degree in Korea University. Her research interests focus on Multimedia, and Information Management and Security.

Hyoung Joong Kim received his B.S., M.S., and Ph.D. degrees from Seoul National University, Seoul, Korea, in 1978, 1986, 1989, respectively. He joined the faculty of the Department of Control and Instrumentation Engineering, Kangwon National University, Korea, in 1989. He is currently a Professor of the Graduate School of Information Management and Security, Korea University, Korea since 2006. His research interests include parallel and distributed computing, multimedia computing, and multimedia security. He contributed to MPEG standardization for Digital Item Adaptation, File Format, Symbolic Music Representation, and Multimedia Application Format with more than 10 contributions and the same number of patents. In addition, he filed many patents and published more than 30 reviewed papers to international journals including IEEE and ACM, and 2 peer-reviewed book chapters. He served as Guest Editor of the IEEE Transactions on Circuits and Systems for Video Technology, EURASIP Journal of Advances in Signal Processing, and Technical Program Chair of many international conferences including International Workshop on Digital Watermarking (IWDW), and so on. He is a Vice Editor-in-Chief of the LNCS Transactions on Data Hiding and Multimedia Security, Associate Editors of well-known international journals, and Editors of many Lecture Notes in Computer Science series. He was the prime investigator of the national projects during 1997-2005 developing interactive and personalized digital television. He is a member of ACM, IEEE and a couple of Korean academic societies.

Joonki Paik was born in Seoul, Korea in 1960. He received the B.S. degree in control and instrumentation engineering from Seoul National University in 1984. He received the M.S. and the Ph.D. degrees in electrical engineering and computer science from Northwestern University in 1987 and 1990, respectively. After getting the Ph.D. degree, he joined Samsung Electronics, where he designed the image stabilization chip sets for consumers camcorders. Since 1993, he has worked for Chung-Ang University, Seoul, Korea, where he is currently a professor in the Department of Image Engineering. From 1999 to 2002, he was a visiting professor at the Department of Electrical and Computer Engineering at the University of Tennessee, Knoxville. He is currently the head of the Image Processing and Intelligent Systems Laboratory, which is supported by the Korean Ministry of Science and Technology under the National Research Laboratory Project, by the Korean Ministry of Education under the Brain Korea 21 Project, and by the Korean Ministry of Information and Communication under ITRC-HNRC.

In-Kwon Yeo received the PhD degree in Statistics from University of Wisconsin-Madison in 1997. He joined the Department of Control and Instrumentation Engineering, Kangwon National University as a visiting professor in 2000 and the Division of Mathematics and Statistical Informatics, Chonbuk National University as an assistant professor in Korea. He is currently an associate professor at the Department of Statistics, Sookmyung Womens University. His current research interests include data transformations, multivariate time series analysis and generalized additive models.